

Trimming the Iterative Fat of Equilibrium Thermodynamic Models Using Neural Networks

Kyle Gorkowski*

Camilo S. Damha, Thomas C. Preston,
Andreas Zuend

Atmospheric and Oceanic Sciences, McGill University

*Now at Los Alamos National Lab, gorkowski@lanl.gov

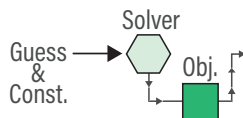
IAMA December, 5 2019



The neural network shortcut

- Iterative solvers can be computationally expensive.

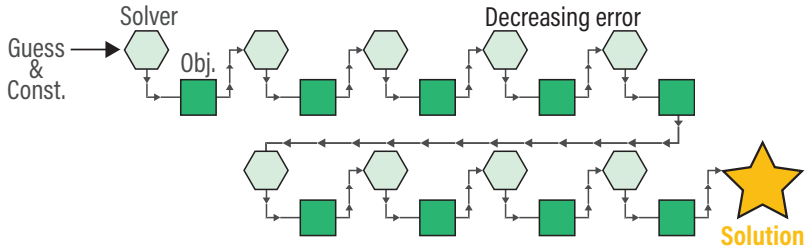
Typical approach



The neural network shortcut

- Iterative solvers can be computationally expensive.
- But, they are transparent and scientifically robust.
- Neural networks are the ultimate black box.

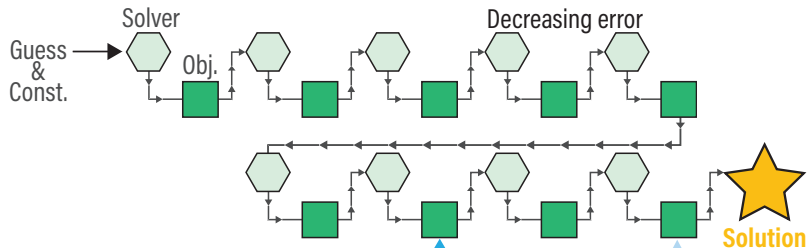
Typical approach



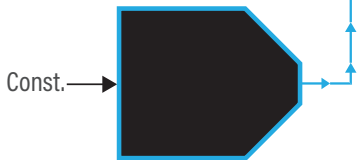
The neural network shortcut

- Iterative solvers can be computationally expensive.
- But, they are transparent and scientifically robust.
- Neural networks are the ultimate black box.
- But, they can be faster than iterative solvers.
- A combined approach is preferable.

Typical approach

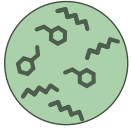


Neural network shortcut



Modeling aerosol mass concentrations ²

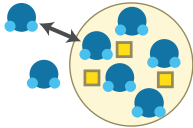
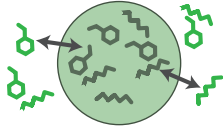
Organics



Inorganic Salts

Emission inventories and chemistry

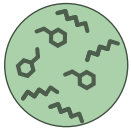
organic vapor equil.



water vapor equil.

Modeling aerosol mass concentrations ²

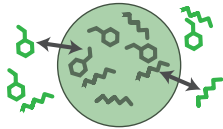
Organics



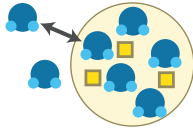
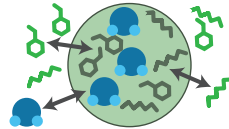
Inorganic Salts

Emission inventories and chemistry

organic vapor equil.

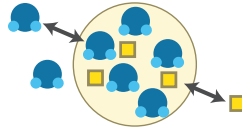


water + org. vapor equil.

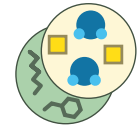
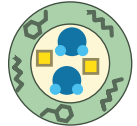
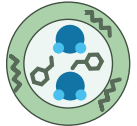


water vapor equil.

water + inorg. vapor equil.



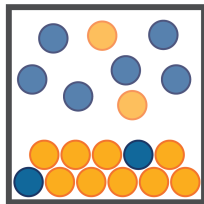
2-phases



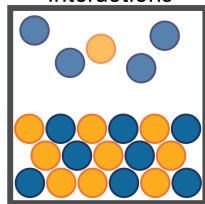
Modified Raoult's law

- Mixing decreases the effective vapor pressure of each component.
- $p_j = p_j^{\text{sat}} x_j \gamma_j = p_j^{\text{sat}} a_j$
- The activity coefficient (γ_j) parameterizes the energetic cost (favorability) of mixing.

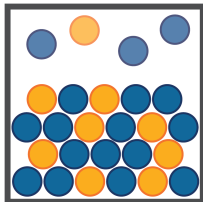
Unfavorable interactions



Ideal (neutral) interactions



Favorable interactions

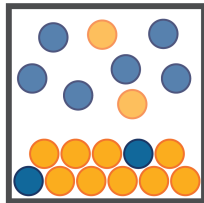


Modified Raoult's law

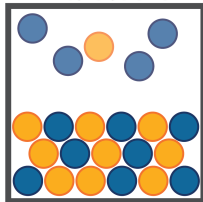
- Mixing decreases the effective vapor pressure of each component.
- $p_j = p_j^{\text{sat}} x_j \gamma_j = p_j^{\text{sat}} a_j$
- The activity coefficient (γ_j) parameterizes the energetic cost (favorability) of mixing.
- In terms of an effective volatility.

$$C_j^* = C_j^{\text{sat}} C_{\Sigma k}^{\Sigma \pi} \frac{\gamma_j q_j^{\pi}}{M_j \sum_k \frac{C_k^{\pi}}{M_k}}$$

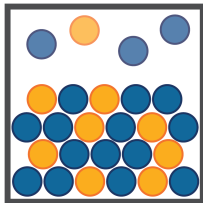
Unfavorable interactions



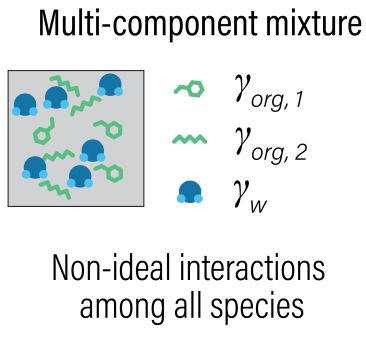
Ideal (neutral) interactions



Favorable interactions

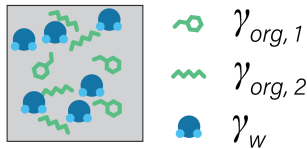


- AIOMFAC is used as a high fidelity reference.



- AIOMFAC is used as a high fidelity reference.
- A simpler Binary Activity Thermodynamics model is built using AIOMFAC generated data.
- github.com/Gorkowski/Binary_Activity_Thermodynamics_Model

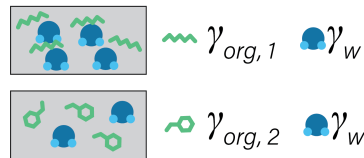
Multi-component mixture



Non-ideal interactions among all species



BAT approximation



Non-ideal interactions with water

- Following a power series expansion of molar excess Gibbs energy of mixing (G^E) (Redlich and Kister, 1948).
- Generalized by parameterizing the expansion coefficients (c_n).
- **Independent variables**
≡ mole fraction (x_{org}) or scaled Vol. (ϕ_{org}), **O:C**, & M_{org}

$$G^E/RT = \phi_{org}(1 - \phi_{org}) [c_1 + c_2(1 - 2\phi_{org})] \quad (1)$$

$$c_n = a_{n,1} \exp(a_{n,2} \times \mathbf{O:C}) + a_{n,3} \exp\left(a_{n,4} \frac{M_w}{M_{org}}\right) \quad (2)$$

- Following a power series expansion of molar excess Gibbs energy of mixing (G^E) (Redlich and Kister, 1948).
- Generalized by parameterizing the expansion coefficients (c_n).
- **Independent variables**
≡ mole fraction (x_{org}) or scaled Vol. (ϕ_{org}), **O:C**, & M_{org}
- **Dependent variables**
☞ water activity ($a_w \times 100\% \approx RH$) and organic activity

$$G^E/RT = \phi_{org}(1 - \phi_{org}) [c_1 + c_2(1 - 2\phi_{org})] \quad (1)$$

$$c_n = a_{n,1} \exp(a_{n,2} \times \text{O:C}) + a_{n,3} \exp\left(a_{n,4} \frac{M_w}{M_{org}}\right) \quad (2)$$

$$\ln(\gamma_w) = (G^E/RT) - x_{org} \frac{d(G^E/RT)}{dx_{org}} \quad (3)$$

$$a_w = \gamma_w(1 - x_{org}) \quad (4)$$

For gas-particle partitioning we need γ_j and $x_{org,j}$; both are used in $C_j^* = C_j^{sat} C_{\Sigma k}^{\Sigma \pi} \frac{\gamma_j q_j^\pi}{M_j \sum_k \frac{C_k^\pi}{M_k}}$.

3-D Models will have:

- O:C
- M_{org}
- $RH \approx a_w \times 100\%$

For gas-particle partitioning we need γ_j and $x_{org,j}$; both are used in $C_j^* = C_j^{sat} C_{\Sigma k}^{\Sigma \pi} \frac{\gamma_j q_j^\pi}{M_j \sum_k \frac{C_k^\pi}{M_k}}$.

3-D Models will have:

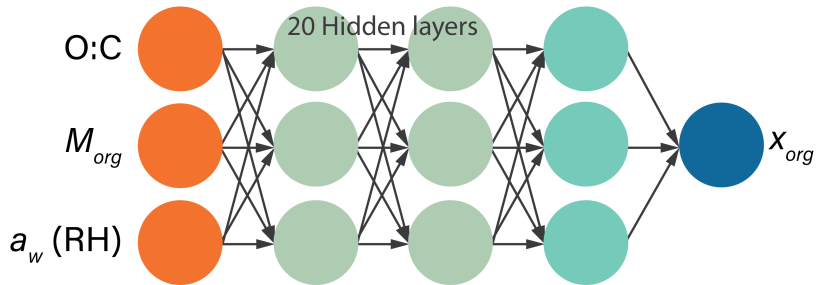
- O:C
- M_{org}
- $RH \approx a_w \times 100\%$

- BAT model must be inverted to use a_w as an input.
- Iterative refinement is possible by varying $x_{org,j}$ to match a_w .
- Instead neural networks are used to directly predict $x_{org,j}$ to a high degree of accuracy.

Building a Neural Network

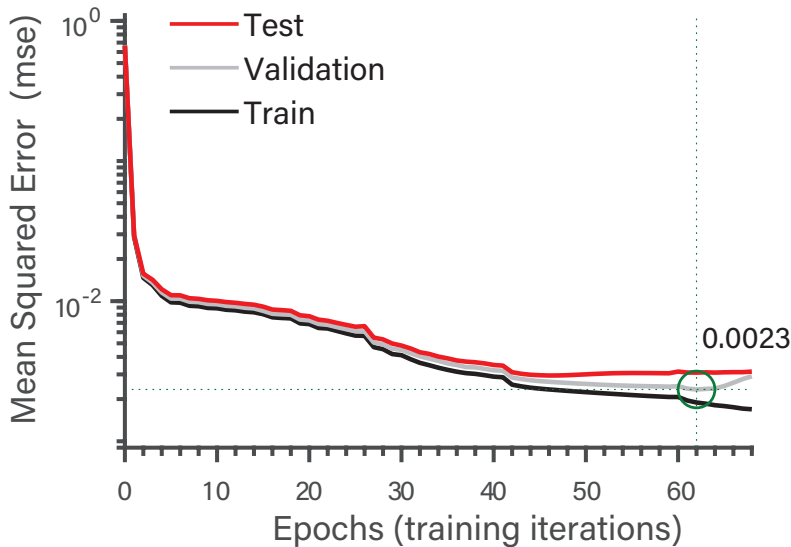
7

- We used a deep belief network of artificial neurons.
- In effect this acts as a generalized curve fitting tool.
- A training database of random inputs and targeted outputs is generated with the BAT model.



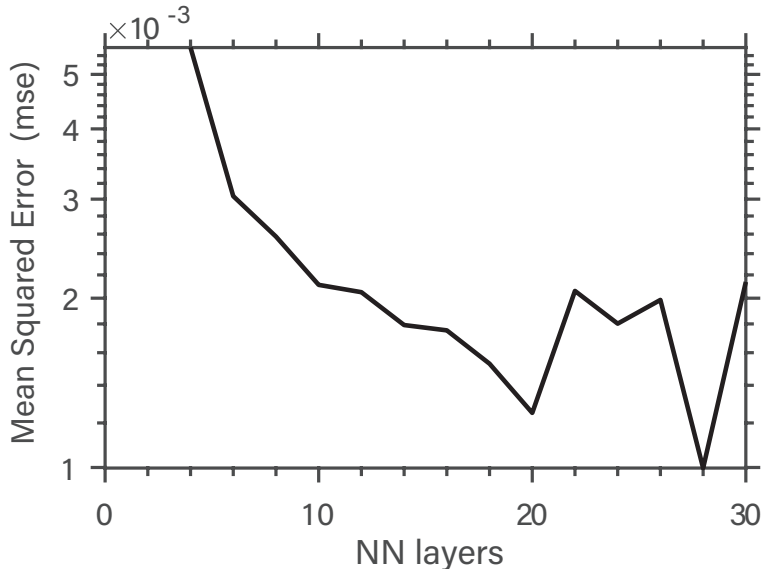
Training of Neural Network

- BAT NN was trained on 9.8×10^6 data points.
- VBS NN was trained on 1.3×10^4 data points.
- Training, validation, and test split of 70/15/15.



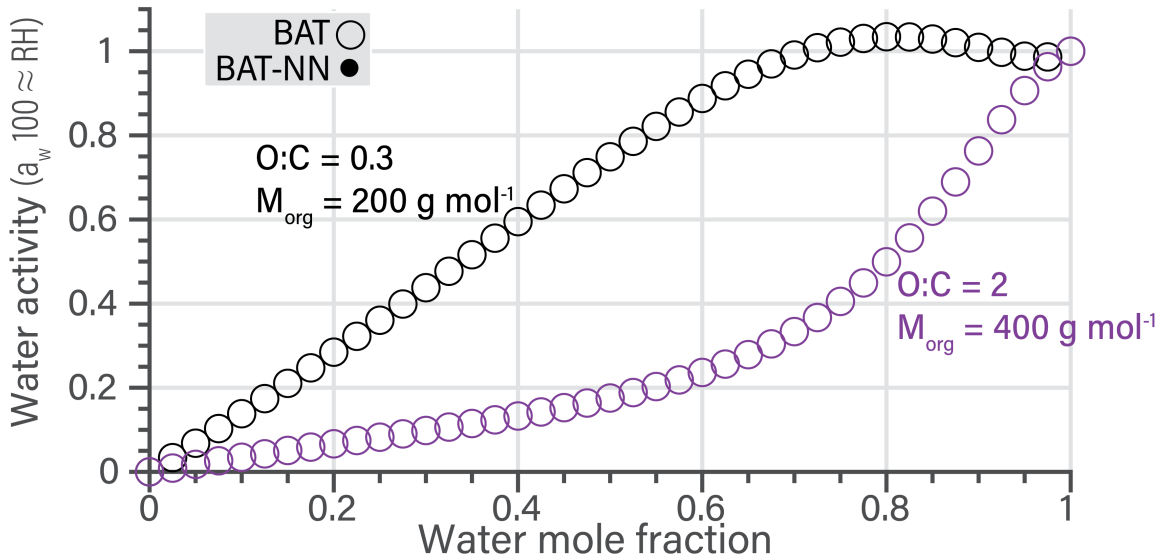
Training of Neural Network

- BAT NN was trained on 9.8×10^6 data points.
- VBS NN was trained on 1.3×10^4 data points.
- Training, validation, and test split of 70/15/15.



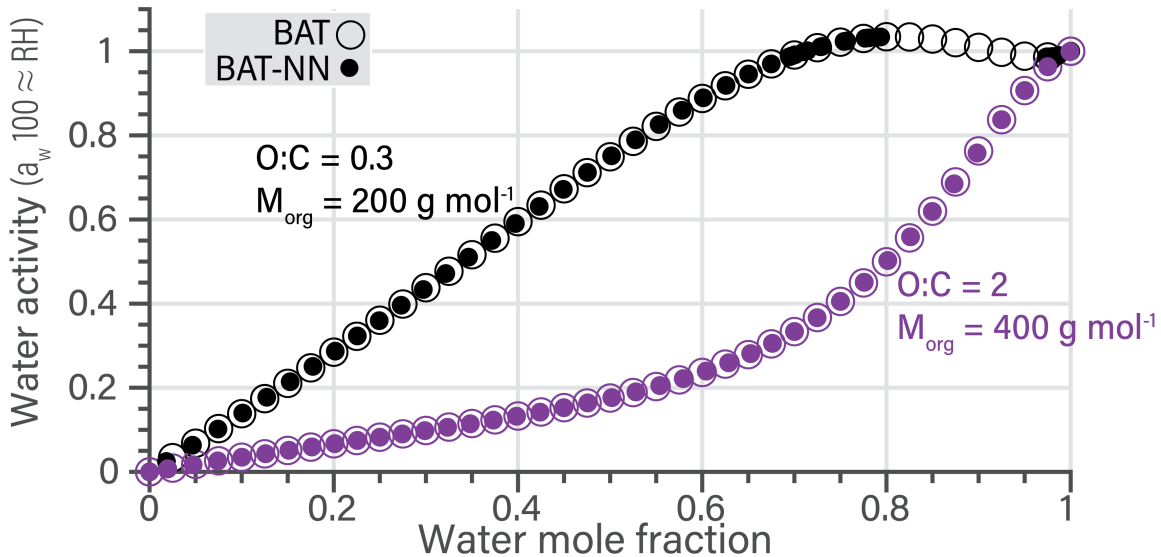
Neural Networks in the context of BAT

9



Neural Networks in the context of BAT

9



Targeting 3-D models (GEOS-Chem)

10

Inputs are a_w , $C_j^{g+\Sigma\pi}$, C_j^{sat} , and chemical information.

Low Fidelity

average molecule functionality,

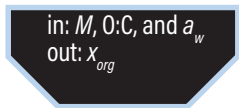
M_{avg} , O:C_{avg}, (H:C_{avg})

High Fidelity

j^{th} molecule functionality,

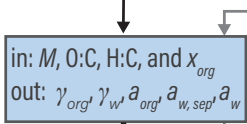
M_j , O:C_j, (H:C_j)

BAT
neural network



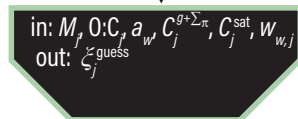
0.13 ms

BAT evaluation
with optional a_w
refinement loop.



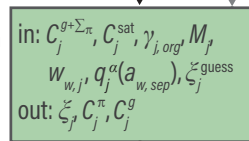
0.58 ms

VBS
neural network



2.8 ms

VBS+BAT evaluation
with equilibrium
solver.



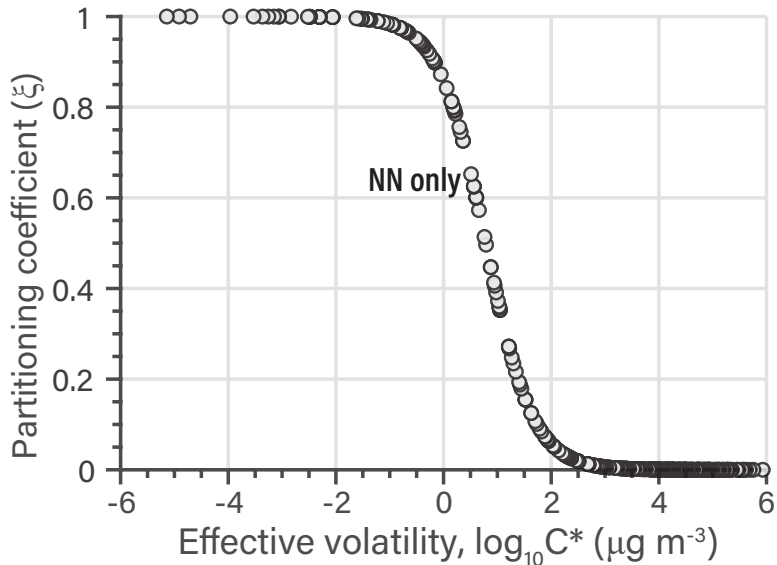
10 ms

Organic and Water PM_{2.5} mass

Isoprene SOA: NN underpredicts

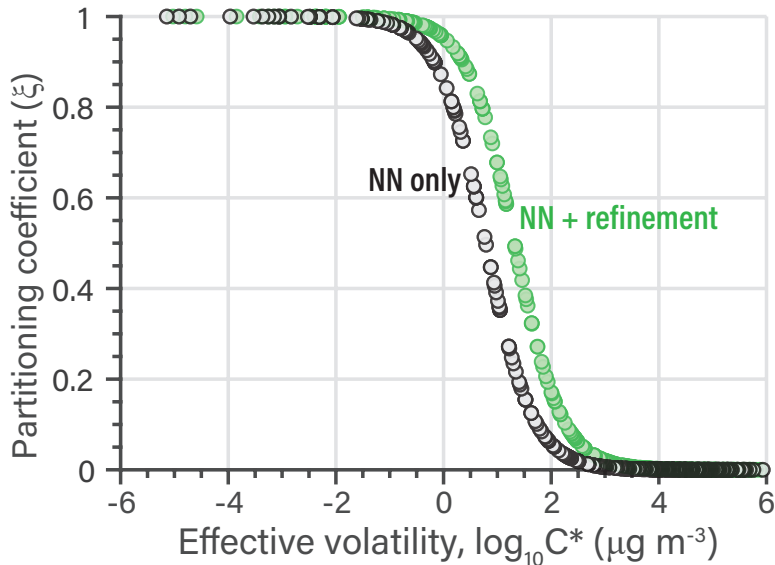
11

- MCM simulation outputs.
- Isoprene and O_3 at 100 ppb.
- Simulation of 343 products after 12 hr.
- Used the EVAPORATION model for vapor pressure estimations.



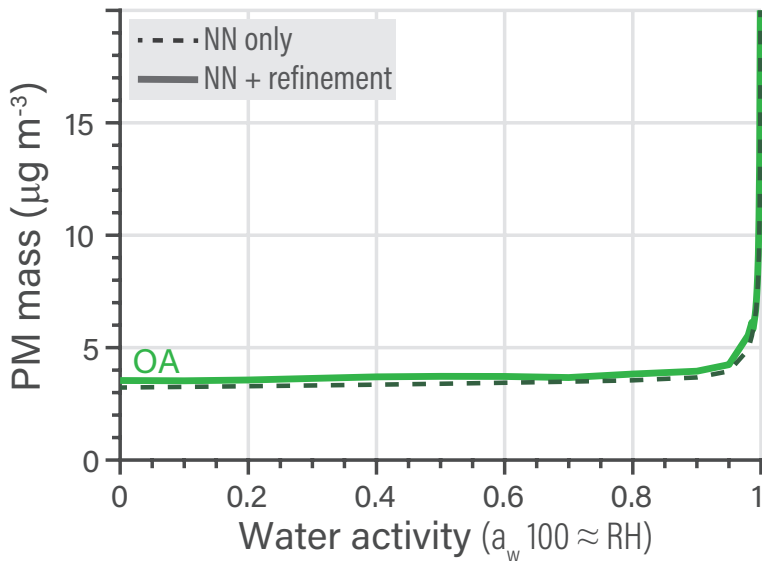
Isoprene SOA: NN underpredicts

- MCM simulation outputs.
- Isoprene and O_3 at 100 ppb.
- Simulation of 343 products after 12 hr.
- Used the EVAPORATION model for vapor pressure estimations.
- NN only was 2x faster.



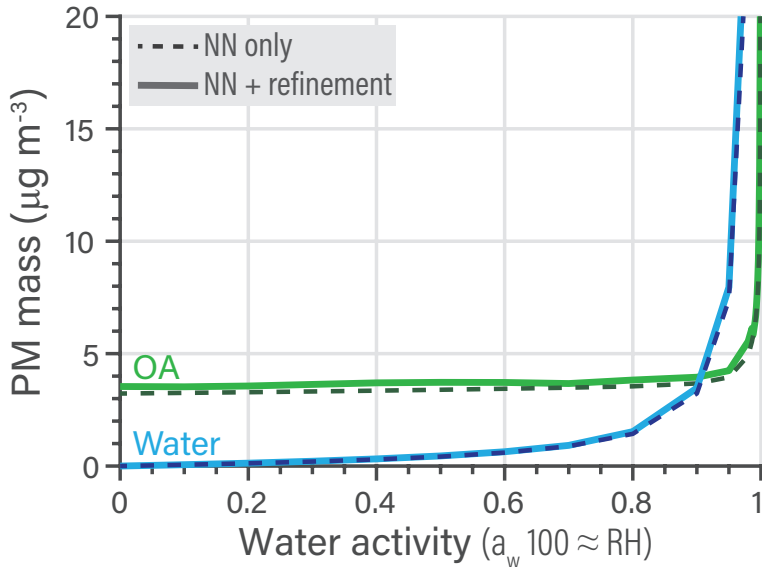
Isoprene SOA: PM mass agrees well

- OA mass agreement is pretty good.



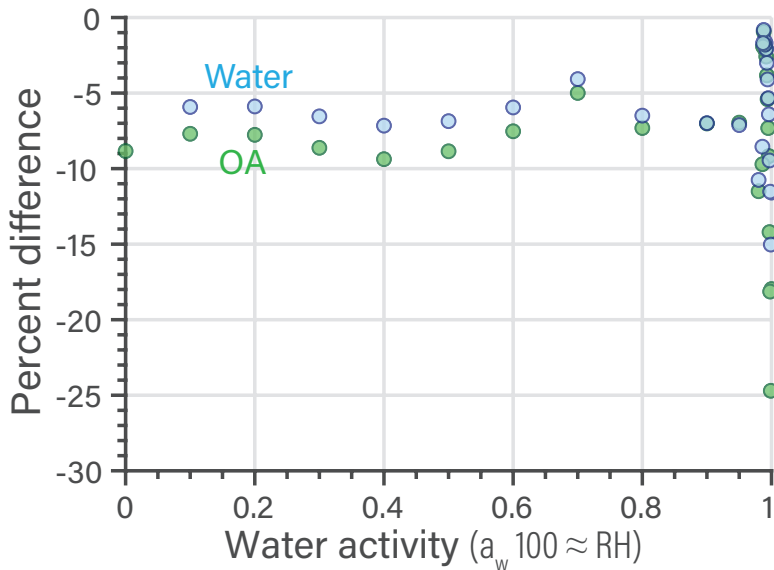
Isoprene SOA: PM mass agrees well

- OA mass agreement is pretty good.
- Aerosol water mass is also in agreement.



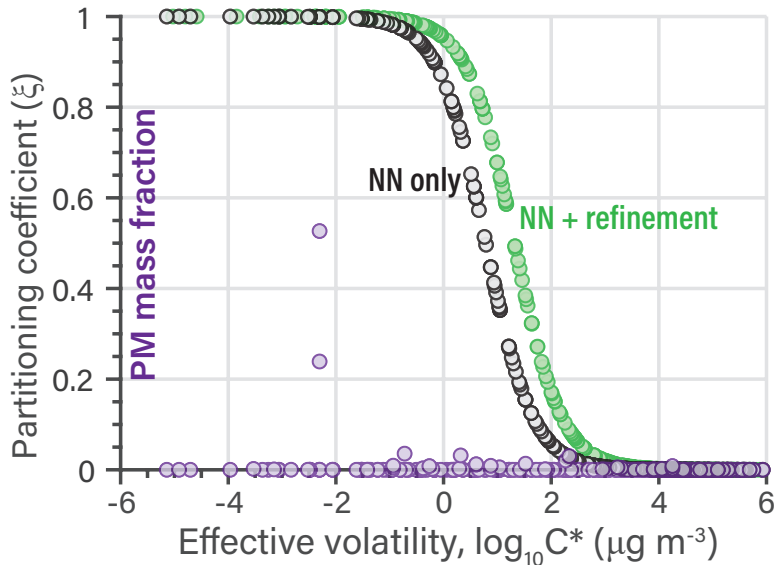
Isoprene SOA: PM mass agrees well

- OA mass agreement is pretty good.
- Aerosol water mass is also in agreement.
- The mass errors are $< 10\%$, except in the CCN activation region.



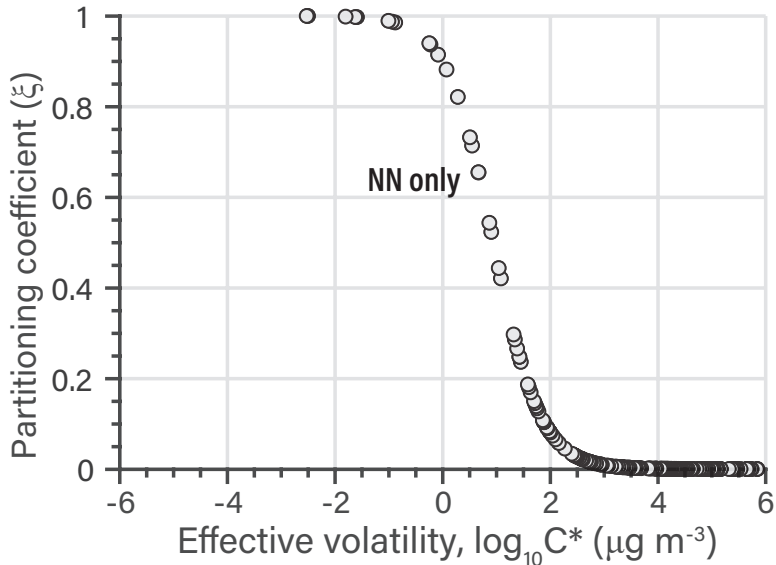
Isoprene SOA: PM mass agrees well

- OA mass agreement is pretty good.
- Aerosol water mass is also in agreement.
- The mass errors are $< 10\%$, except in the CCN activation region.
- The errors in partitioning coefficients are not directly translated to PM mass errors.



α -Pinene SOA: NN underpredicts

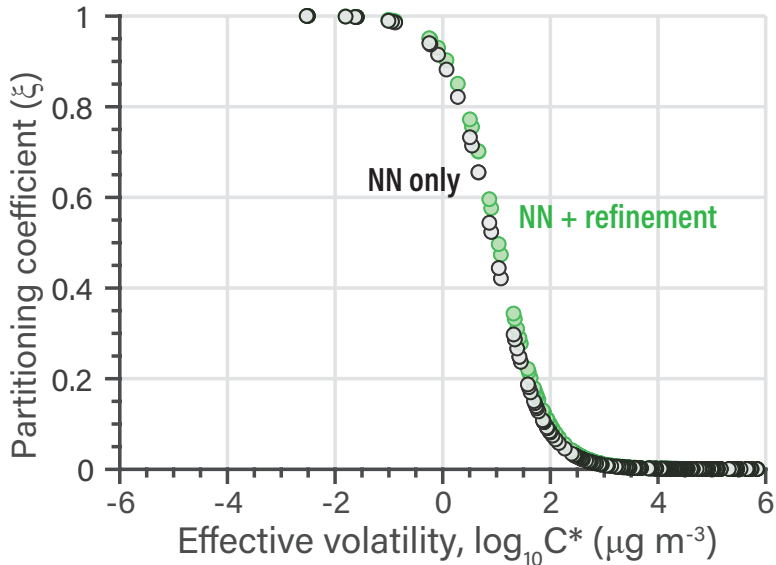
- α -Pinene and O_3 at 20 ppb.
- Simulation of 198 products after 12 hr.



α -Pinene SOA: NN underpredicts

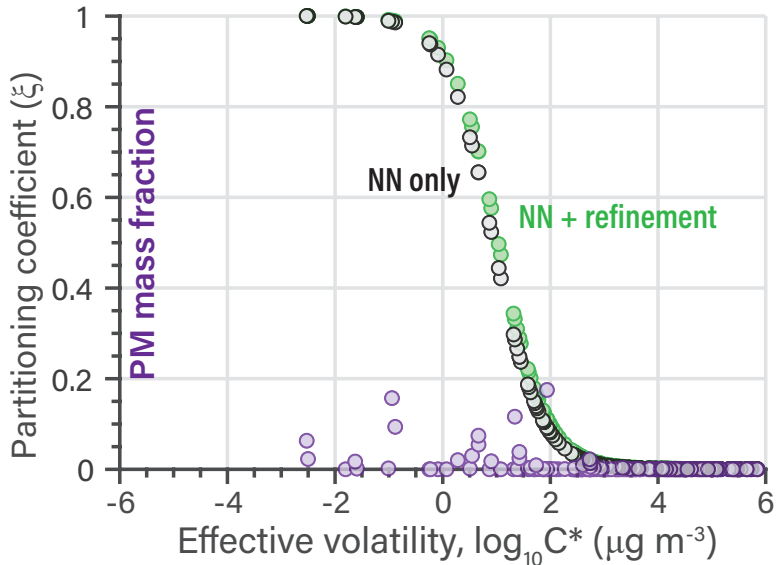
13

- α -Pinene and O_3 at 20 ppb.
- Simulation of 198 products after 12 hr.
- NN only was 1.5x faster.
- NN+refinement was 2-5 times faster than iterative refinement only.

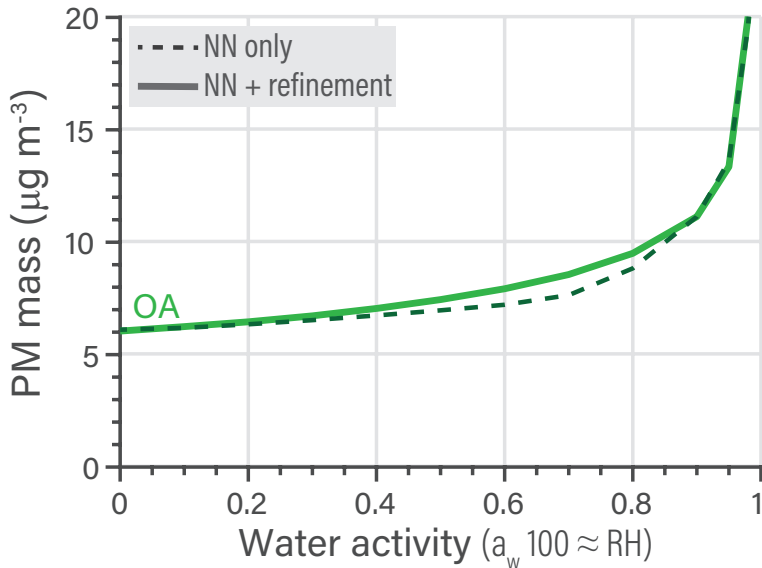


α -Pinene SOA: NN underpredicts

- α -Pinene and O_3 at 20 ppb.
- Simulation of 198 products after 12 hr.
- NN only was 1.5x faster.
- NN+refinement was 2-5 times faster than iterative refinement only.

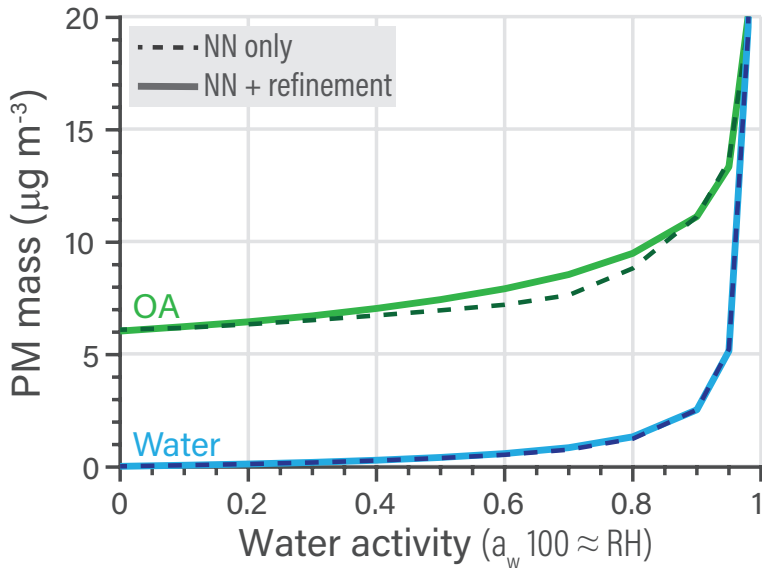


■ Good mass agreement.



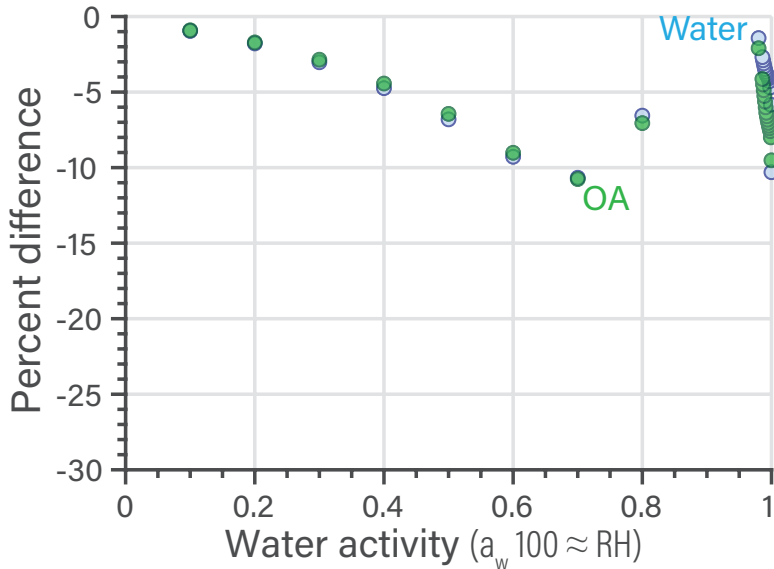
α -Pinene SOA: PM mass agrees well

■ Good mass agreement.



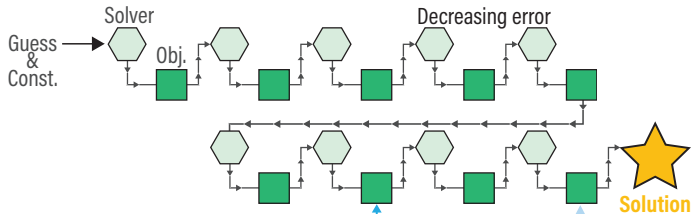
α -Pinene SOA: PM mass agrees well

- Good mass agreement.
- The mass errors are < 11%.

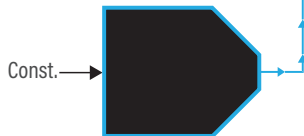


- The combination of iterative solvers and NN can be accurate and efficient.

Typical approach

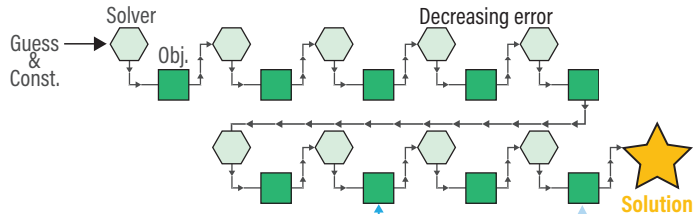


Neural network shortcut

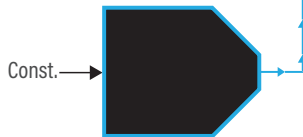


- The combination of iterative solvers and NN can be accurate and efficient.
- Extensions of this methodology to other processes, is possible as long as the computation trade-off is favorable.

Typical approach

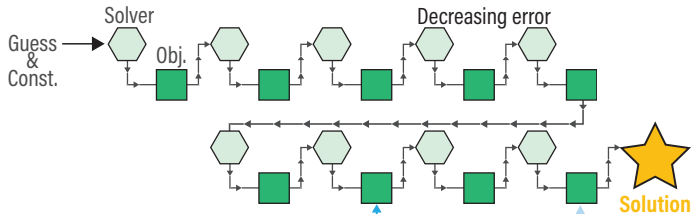


Neural network shortcut

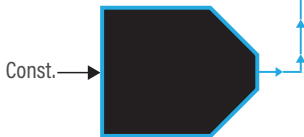


- The combination of iterative solvers and NN can be accurate and efficient.
- Extensions of this methodology to other processes, is possible as long as the computation trade-off is favorable.
- Extensions to the BAT model will look at organic-organic and inorganic-organic equilibrium modeling.

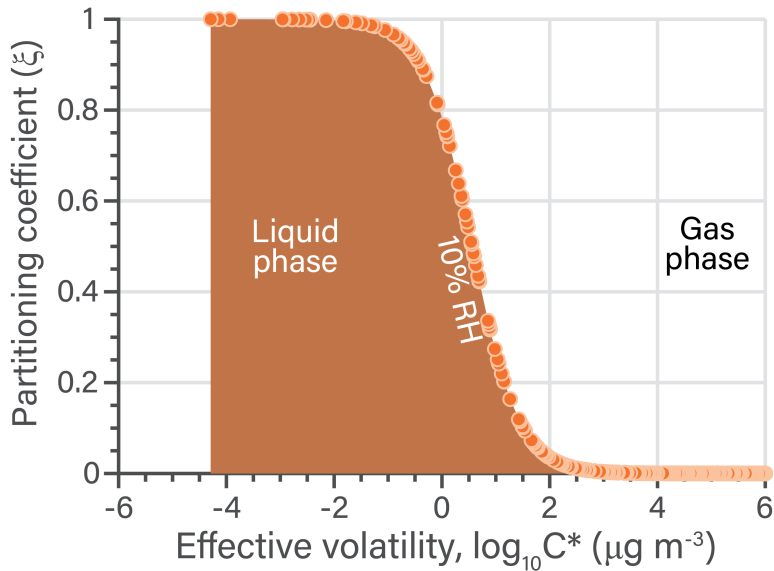
Typical approach



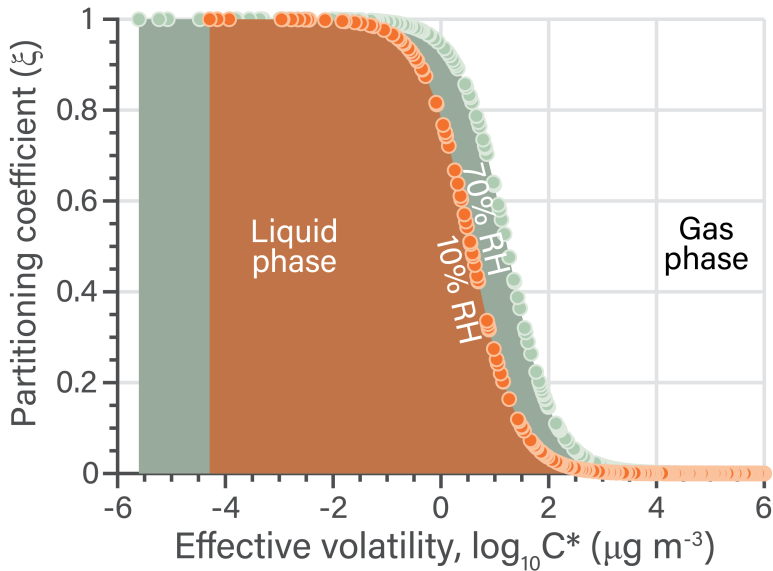
Neural network shortcut



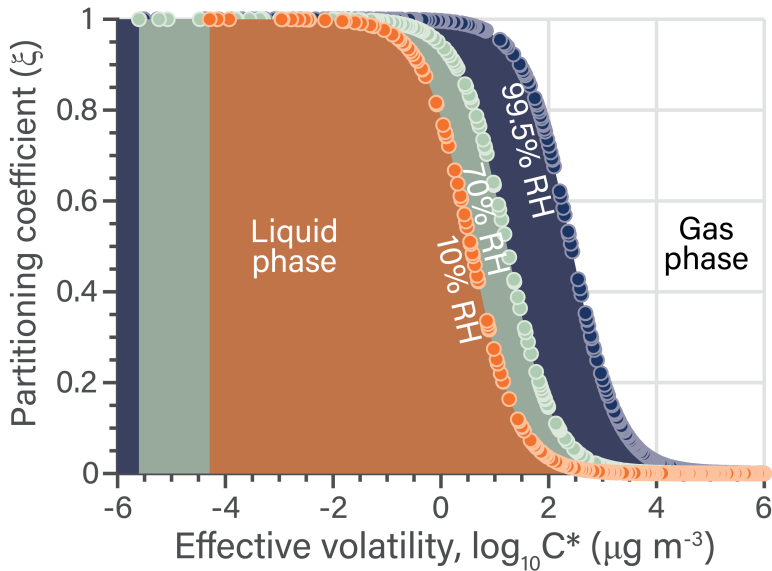
Volatility is dependent on RH



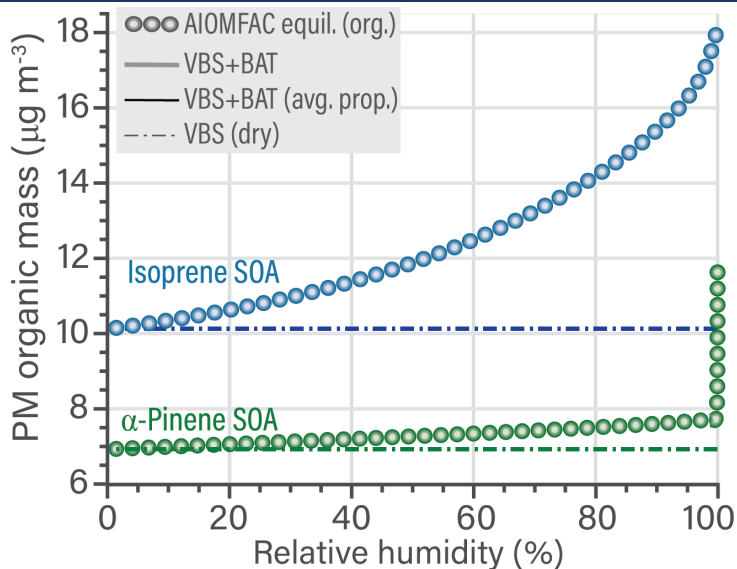
Volatility is dependent on RH



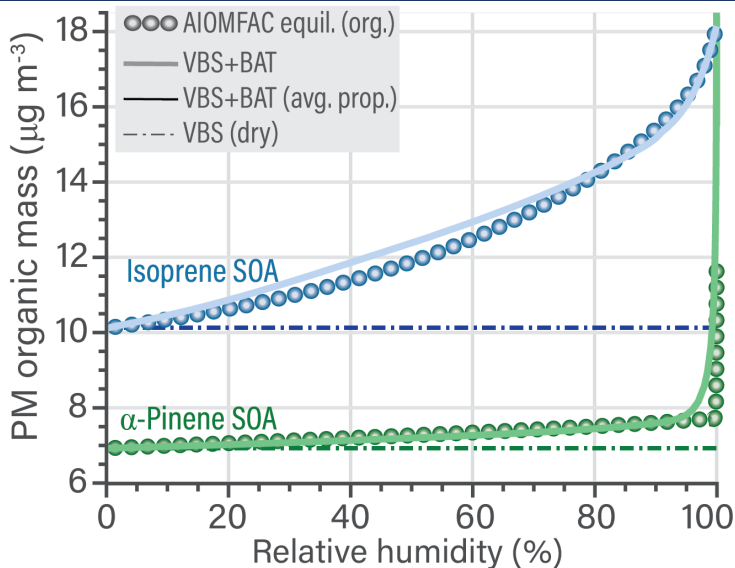
Volatility is dependent on RH



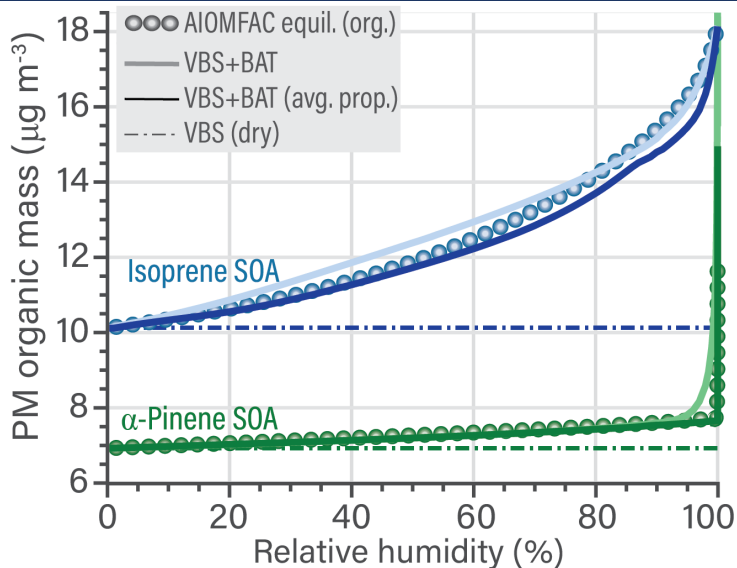
Organic mass shows good agreement



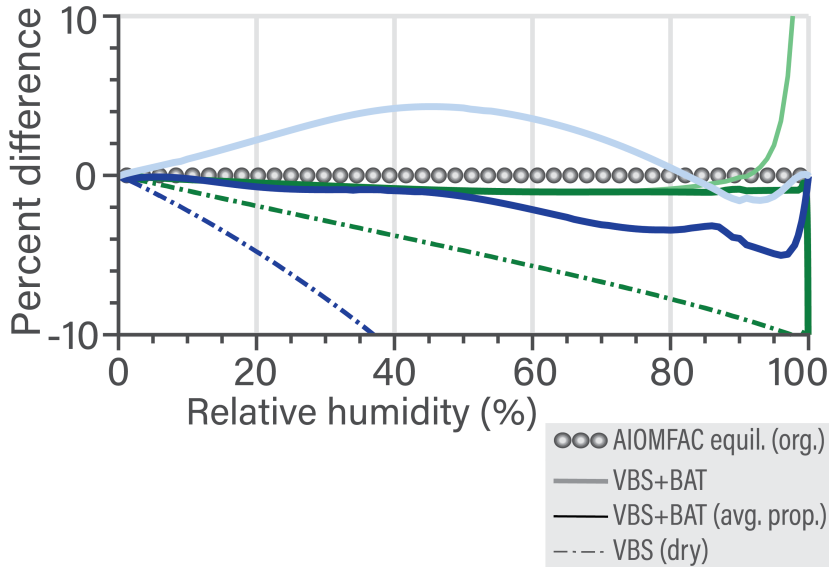
Organic mass shows good agreement



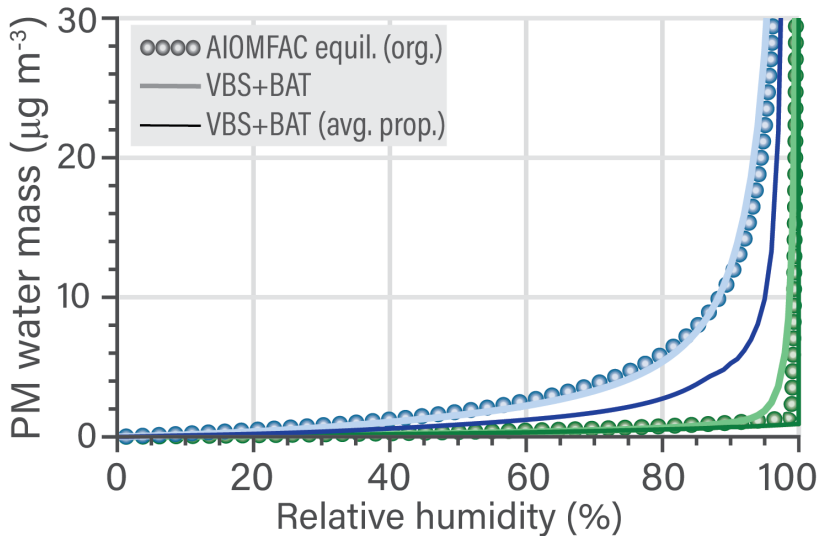
Organic mass shows good agreement



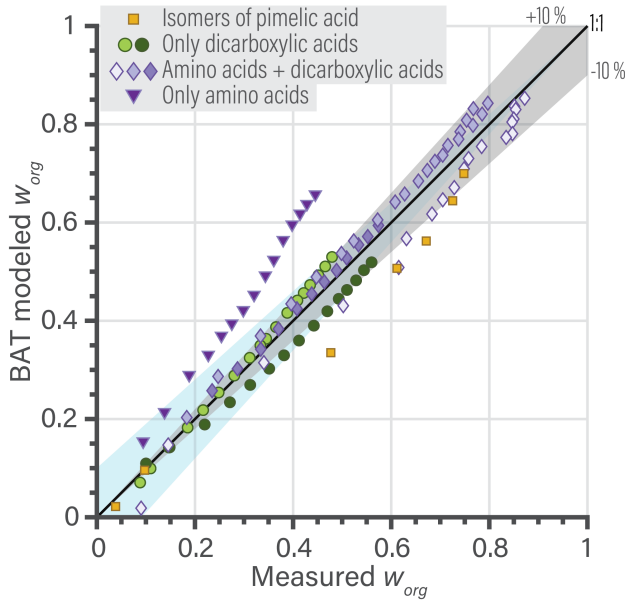
Organic mass shows good agreement



Water mass also agrees

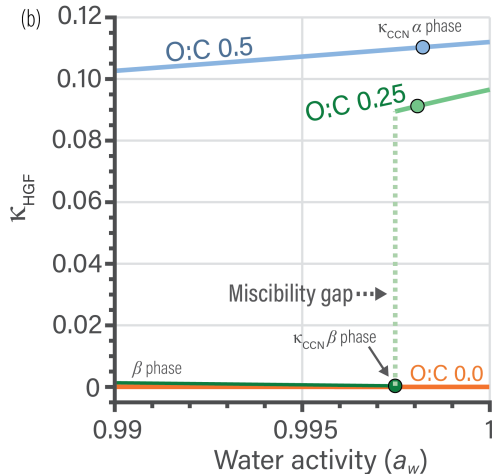
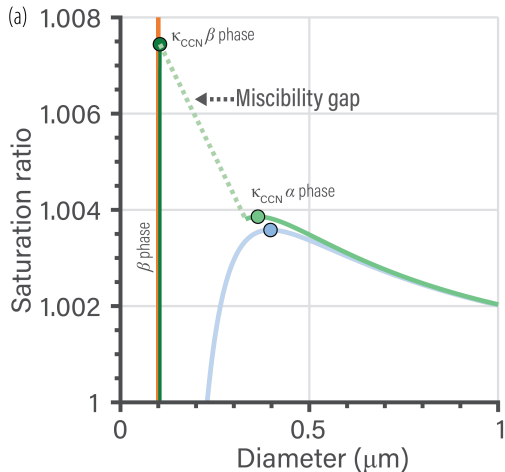


Measurement agreement of organic mass fractions



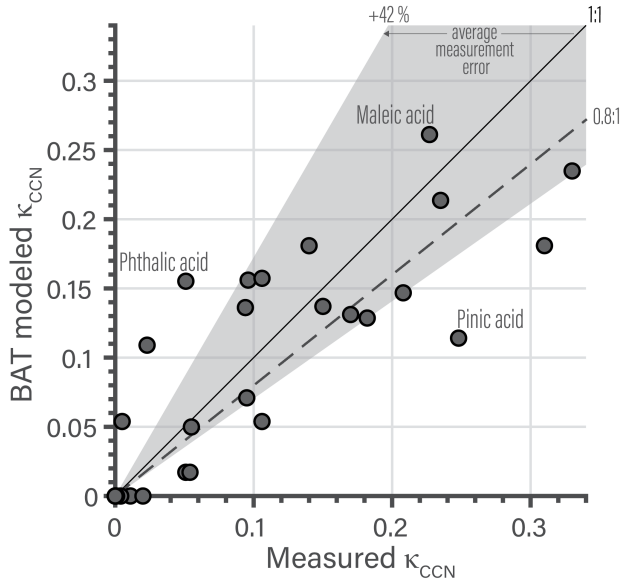
Side note on Köhler curves of CCN

$$\frac{1}{a_w} = 1 + \kappa_{HGF} \frac{V_{org, dry}}{V_w + V_{org} - V_{org, dry}}$$

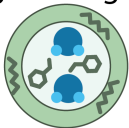


Measurement agreement: κ_{CCN}

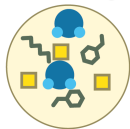
- 30 comparison points
- Error of ± 0.055



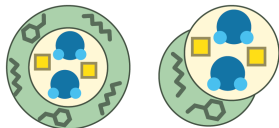
Organic-organic interactions



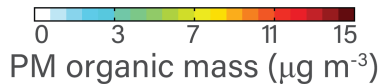
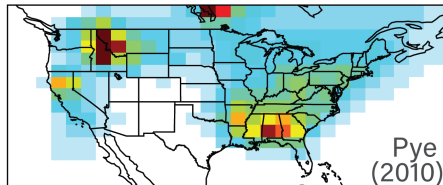
Inorganic-organic interactions



2-Phase systems



Camilo is pursuing the implementation into GEOS-Chem.



- Gorkowski, K., Preston, T. C., and Zuend, A.: RH-dependent organic aerosol thermodynamics via an efficient reduced-complexity model, *Atmos. Chem. Phys. Discuss.*, pp. 1–37, <https://doi.org/10.5194/acp-2019-495>, URL <https://www.atmos-chem-phys-discuss.net/acp-2019-495/>, 2019.
- Redlich, O. and Kister, A. T.: Algebraic Representation of Thermodynamic Properties and the Classification of Solutions, *Ind. Eng. Chem.*, 40, 345–348, <https://doi.org/10.1021/ie50458a036>, 1948.